

RAPID COMMUNICATION

Nanocomposite (Nd,Dy)(Fe,Co,Nb,B)_{5.5}/α-Fe multilayer magnets with high performance

W Liu^{1,2,5,6}, Z D Zhang¹, J P Liu^{2,3}, Z R Dai⁴, Z L Wang⁴,
X K Sun¹ and D J Sellmyer²

¹ Shenyang National Laboratory for Materials Science, Institute of Metal Research, Chinese Academy of Sciences, Shenyang 110016, People's Republic of China

² Center for Materials Research and Analysis, University of Nebraska, Lincoln, NE 68588-0113, USA

³ Institute for Micromanufacturing, Louisiana Tech University, Ruston, LA 71272, USA

⁴ School of Materials Science and Engineering, Georgia Institute of Technology, Atlanta, GA 30332-0245, USA

E-mail: wliu@imr.ac.cn

Received 10 March 2003, in final form 20 June 2003

Published 22 August 2003

Online at stacks.iop.org/JPhysD/36/L67

Abstract

The structural and magnetic properties of rare-earth nanocomposite magnets of a (Nd,Dy)(Fe,Co,Nb,B)_{5.5} single layer and a (Nd,Dy)(Fe,Co,Nb,B)_{5.5}/α-Fe multilayer prepared by sputtering and heat treatment have been investigated. Incomplete exchange coupling behaviour is observed in the Ti-buffered NdDyFeCoNbB + 40 wt%Fe single layer magnet. After annealing, the laminated nanostructure consisting of mutually dispersed soft and hard phases results in remanence enhancement. The optimum magnetic properties of $J_r = 1.11$ T, $\mu_{0i} H_c = 0.88$ T and $(BH)_{\max} = 192$ kJ m⁻³ are achieved in the multilayer magnet annealed at 550°C for 30 min. The designed multilayer film with thinner soft magnetic layers may favour the formation of more ideal nanostructures for exchange coupling between soft- and hard-magnetic phases.

Experimental researches on nanostructured exchange-coupled magnets have been performed since 1988 [1]. Taking advantage of high coercivity and high magnetization contributed by hard- and soft-magnetic components, respectively, high remanence and a large maximum energy product would be obtained if a full exchange coupling existing between the grains of the two phases in nanocomposite magnets, as predicted based on micromagnetic calculation [2–4]. However, up to now, the energy products of the rare-earth nanocomposite magnets prepared by means of rapid quenching and mechanical alloying have been much lower than the theoretical expectation, due to difficulties in controlling the nanostructures [5–8].

⁵ Also at: International Centre for Materials Physics, Chinese Academy of Sciences, Shenyang 110016, People's Republic of China.

⁶ Author to whom any correspondence should be addressed.

Recently, some studies on exchange coupling were carried out for nanostructured CoSm/FeCo and PrCo/Co multilayers prepared by sputtering and subsequent heat treatment [9, 10]. The magnetic properties of exchange-coupled α-Fe/Nd-Fe-B multilayer magnets were investigated by Shindo [11] and observations for Nd-Fe-B/Fe/Nd-Fe-B trilayers were reported by Parhofer and Yang *et al* [12–14]. In our previous study [15], we investigated the magnetic properties of nanocomposite multilayer magnets of NdDyFeCoNbB/M (M = Co, Fe₆₅Co₃₅) on Ti-buffered Si substrates prepared by sputtering and subsequent heat treatment. In comparison with the single layer, the remanence of the multilayer magnets was found to increase noticeably. In this letter, we report the structural and magnetic properties of nanocomposite (Nd,Dy)(Fe,Co,Nb,B)_{5.5}/Fe multilayer magnets synthesized

by sputtering and subsequent annealing. High permanent-magnet performance is obtained with optimum magnetic properties $J_r = 1.11$ T, $\mu_{0i}H_c = 0.88$ T and $(BH)_{\max} = 192$ kJ m⁻³ for a rare-earth multilayer magnet annealed at 550°C for 30 min.

(Nd,Dy)(Fe,Co,Nb,B)_{5.5}/α-Fe thin films were prepared with a multiple-gun dc- and rf-sputtering system by depositing (Nd_{0.9}Dy_{0.1})(Fe_{0.77}Co_{0.12}Nb_{0.03}B_{0.08})_{5.5} alloy and Fe onto silicon substrates, covered with a 10 or 20 nm Ti-buffer. The alloy target was home-made by sintering powdered compacts, and other targets were commercial products. Purity of all the targets was higher than 99.9%. The base pressure of the sputtering system was $(2-3) \times 10^{-7}$ Torr, and the Ar pressure during the sputtering was 5 mTorr. The thickness of the films was measured by weighing them. The as-deposited films were annealed in a furnace with a vacuum of 2×10^{-7} Torr. The crystalline structure of the phases in the films was identified by x-ray diffractometry with Cu Kα radiation, and by transmission electron microscopy (TEM). The magnetic properties of the films were measured by an alternating gradient force magnetometer (AGFM) and a superconducting quantum interference device (SQUID) magnetometer. The measuring field is applied in the plane of the film and the bulk demagnetizing coefficient is effectively zero.

X-ray diffraction (XRD) patterns of the different nanocomposite films are shown in figure 1, where figure 1(a) corresponds to a Ti-buffered NdDyFeCoNbB+40wt%Fe single layer with a thickness of 640 nm on the Si substrate annealed at 600°C for 5 min; (b) a Ti(20 nm)/[NdDyFeCoNbB(16 nm)Fe(7.5 nm)] × 10/Ti(20 nm)/(Si substrate) multilayer annealed at 600°C for 20 min; (c) a Ti(10 nm)/[NdDyFeCoNbB(16 nm)Fe(1.5 nm)] × 20/Ti(10 nm)/(Si substrate) multilayer annealed at 550°C for 30 min. It is seen that the hard-magnetic phase of Nd₂Fe₁₄B-type coexists with a large amount of α-Fe,

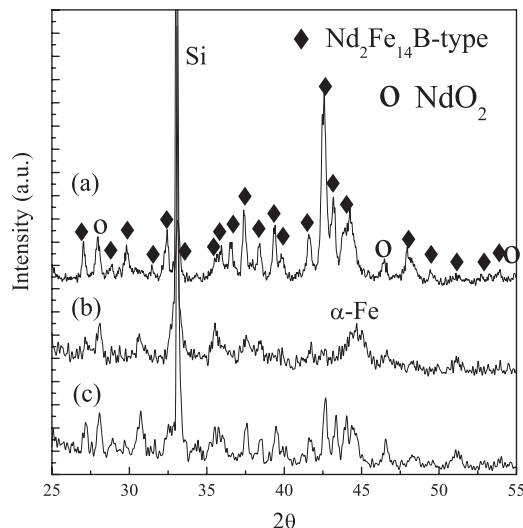


Figure 1. XRD patterns for (a) a Ti-buffered NdDyFeCoNbB + 40 wt%Fe single layer with a thickness of 640 nm on the Si substrate annealed at 600°C for 5 min; (b) a Ti(20 nm)/[NdDyFeCoNbB(16 nm)Fe(7.5 nm)] × 10/Ti(20 nm)/(Si substrate) multilayer annealed at 600°C for 20 min; (c) a Ti(10 nm)/[NdDyFeCoNbB(16 nm)Fe(1.5 nm)] × 20/Ti(10 nm)/(Si substrate) multilayer annealed at 550°C for 30 min.

accompanied by a trace quantity of NdO₂. The XRD profiles of the films reveal a random orientation of the grains of the Nd₂Fe₁₄B-type phase.

The investigation on the hard-magnetic single layer was reported in our previous paper, and the as-deposited film on the Si substrate of Ti-buffered NdDyFeCoNbB is amorphous [15]. After annealing at 625°C for 5 min, the magnetically hard phase in the film is of the Nd₂Fe₁₄B-type [15]. To prepare a nanocomposite single layer comprising both the soft and hard phases, an alloy target with the composition (Nd_{0.9}Dy_{0.1})(Fe_{0.77}Co_{0.12}Nb_{0.03}B_{0.08})_{5.5} plus 40 wt% α-Fe was prepared. All the magnetic measurements were carried out along the film planes. The hysteresis loop at room temperature of the Ti-buffered NdDyFeCoNbB + 40 wt%Fe single layer on the Si substrate annealed at 600°C for 5 min, which has a film thickness of 640 nm, is shown in figure 2. A clear ‘shoulder’ on the hysteresis loop is observed, due to deficient exchange coupling between the soft and hard phases. Thus, after annealing, although the hard-magnetic 2 : 14 : 1 phase and soft-magnetic α-Fe phase apparently coexist in the film, according to the XRD pattern (see figure 1), the distribution of the two phases may not be homogeneous in the film, and the averaged grain size of the soft-magnetic α-Fe phase is much larger than the optimum one for exchange coupling. Non-uniform clustering of α-Fe is not favourable for exchange coupling between the hard and soft phases, resulting in poor permanent-magnetic properties in the nanocomposite single layer.

To obtain a more ideal structure with a uniform distribution of the soft and hard phases, a multilayer with the structure Ti(20 nm)/[NdDyFeCoNbB(16 nm)Fe(7.5 nm)] × 10/Ti(20 nm)/(Si substrate) was prepared by sputtering. Hysteresis loops at room temperature of Ti(20 nm)/[NdDyFeCoNbB(16 nm)Fe(7.5 nm)] × 10/Ti(20 nm)/(Si substrate) multilayer and Ti(20 nm)/[NdDyFeCoNbB(16 nm)Fe(7.5 nm)] × 10/Ti(20 nm)/(Si substrate) multilayer and Ti(20 nm)/[NdDyFeCoNbB(16 nm)Fe(7.5 nm)] × 10/Ti(20 nm)/(Si substrate) multilayer annealed at 600°C for 20 min are shown in figure 3. The magnetic properties of the hard-phase single layer are $J_r = 0.58$ T, $\mu_{0i}H_c = 1.32$ T

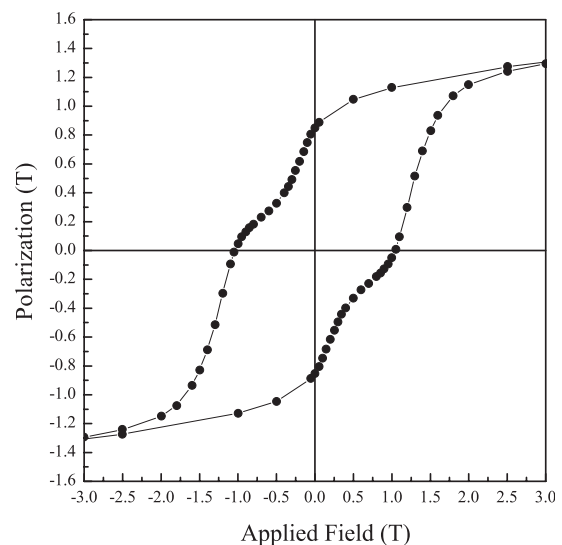


Figure 2. Room temperature hysteresis loops of a Ti-buffered NdDyFeCoNbB + 40 wt%Fe single layer with a thickness of 640 nm on the Si substrate annealed at 600°C for 5 min.

and $(BH)_{\max} = 46.3 \text{ kJ m}^{-3}$; while those of the nanocomposite multilayer are $J_r = 0.95 \text{ T}$, $\mu_{0i} H_c = 0.91 \text{ T}$ and $(BH)_{\max} = 114 \text{ kJ m}^{-3}$. Although the remanence and the maximum energy product are greatly enhanced due to improved exchange coupling in comparison with the results for the hard-phase single layer and the nanocomposite single layer mentioned above, the squareness of the hysteresis loop for the multilayer is not good enough and thus the energy product is not high.

Figure 4 shows a TEM bright-field image of the $\text{Ti}(20 \text{ nm})/[\text{NdDyFeCoNbB}(16 \text{ nm})\text{Fe}(7.5 \text{ nm})] \times 10/\text{Ti}(20 \text{ nm})/(\text{Si substrate})$ multilayer annealed at 600°C for 20 min. It is shown that the laminated structure consisting of the soft- and hard-magnetic components exists in the multilayer, and the magnetically soft iron layer has not been completely segregated by the hard-magnetic component. The hard-magnetic phase with the $\text{Nd}_2\text{Fe}_{14}\text{B}$ -type structure with

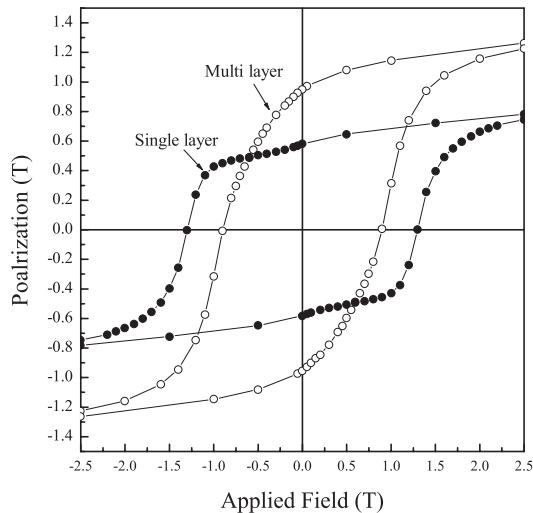


Figure 3. Room temperature hysteresis loops of a $\text{Ti}(20 \text{ nm})/[\text{NdDyFeCoNbB}(16 \text{ nm})\text{Fe}(7.5 \text{ nm})] \times 10/\text{Ti}(20 \text{ nm})/(\text{Si substrate})$ multilayer and a $\text{Ti}(20 \text{ nm})/[\text{NdDyFeCoNbB}(160 \text{ nm})]/\text{Ti}(20 \text{ nm})/(\text{Si substrate})$ annealed at 600°C for 20 min.

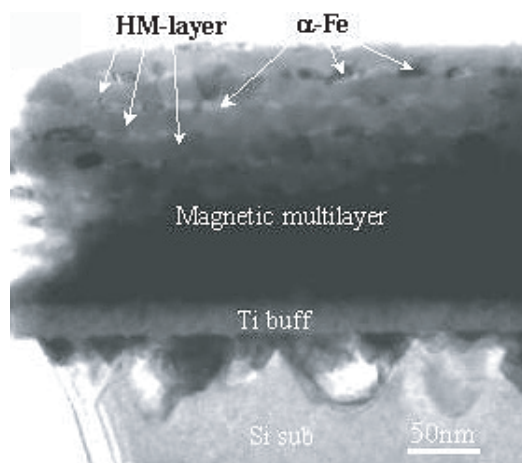


Figure 4. TEM bright-field image of the $\text{Ti}(20 \text{ nm})/[\text{NdDyFeCoNbB}(16 \text{ nm})\text{Fe}(7.5 \text{ nm})] \times 10/\text{Ti}(20 \text{ nm})/(\text{Si substrate})$ multilayer thin film annealed at 600°C for 20 min.

spread peaks and $\alpha\text{-Fe}$ is observed in the XRD patterns (see figure 1). It is concluded that crystallization of the $\text{Nd}_2\text{Fe}_{14}\text{B}$ -type phase is not complete. In the as-deposited multilayer film of our previous paper [16], the distribution of the soft Fe layer and the hard phase layer in the amorphous state was very uniform (see the cross-sectional view TEM image in figure 1 of [16]). After annealing at appropriate temperatures, as shown in the plan-view elemental maps of figures 3(a) and (b) in [16], the well-designed multilayer films consisted of a magnetically hard $\text{Nd}_2\text{Fe}_{14}\text{B}$ -type phase with a grain size of 40 nm and a soft $\alpha\text{-Fe}$ phase in the form of continuous layers [16]. Similarly, as shown in figure 4, the magnetically soft $\alpha\text{-Fe}$ phase of the present multilayer film also exists in the form of continuous layers. In this case, after annealing, the elements in the two layers with two different phases do not completely diffuse into each other. Although the final microstructure of the multilayer film is not ideal, the laminated nanostructure consisting of mutually dispersed soft and hard phases can still result in the enhancement of remanent polarization.

To obtain better results on magnetic properties in multilayer films, a multilayer film with more thin Fe layers was prepared. The hysteresis loops at room temperature of the $\text{Ti}(10 \text{ nm})/[\text{NdDyFeCoNbB}(16 \text{ nm})\text{Fe}(1.5 \text{ nm})] \times 20/\text{Ti}(10 \text{ nm})/(\text{Si substrate})$ multilayer annealed at 550°C and 575°C for 30 min and the $\text{Ti}(10 \text{ nm})/[\text{NdDyFeCoNbB}(320 \text{ nm})]/\text{Ti}(10 \text{ nm})/(\text{Si substrate})$ single layer annealed at 550°C for 30 min are given in figure 5. The best magnetic properties of $J_r = 0.64 \text{ T}$, $\mu_{0i} H_c = 1.3 \text{ T}$ and $(BH)_{\max} = 70.8 \text{ kJ m}^{-3}$, and $J_r = 1.11 \text{ T}$, $\mu_{0i} H_c = 0.88 \text{ T}$ and $(BH)_{\max} = 192 \text{ kJ m}^{-3}$ were achieved in the hard-phase single layer and the nanocomposite multilayer annealed at 550°C for 30 min, respectively. The energy product of the nanocomposite multilayer annealed at 575°C for 30 min is about 166 kJ m^{-3} . Compared with the results for the single layer, remanence enhancement and a large maximum energy product in the nanocomposite multilayer are obtained, which are

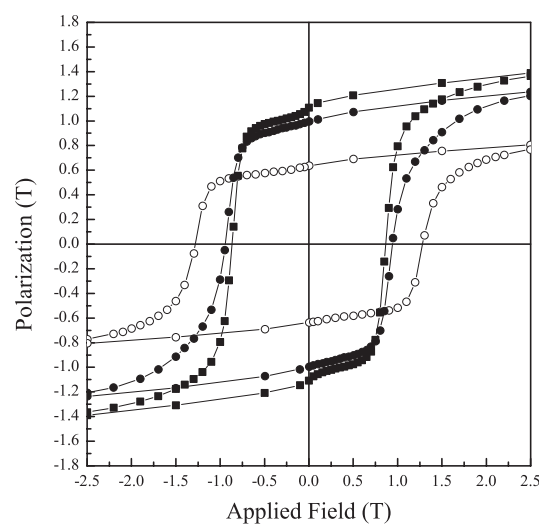


Figure 5. Room temperature hysteresis loops of a $\text{Ti}(10 \text{ nm})/[\text{NdDyFeCoNbB}(16 \text{ nm})\text{Fe}(1.5 \text{ nm})] \times 20/\text{Ti}(10 \text{ nm})/(\text{Si substrate})$ multilayer annealed at (■) 550°C and (●) 575°C for 30 min and a $\text{Ti}(10 \text{ nm})/[\text{NdDyFeCoNbB}(320 \text{ nm})]/\text{Ti}(10 \text{ nm})/(\text{Si substrate})$ layer annealed at (○) 550°C for 30 min.

attributed to exchange coupling between the nano-grains of the soft and hard phases. It is clear that the multilayer film designed with a thinner soft magnetic layer may be favourable for the formation of nanostructure more favourable for exchange coupling between the soft and hard phases.

In summary, we prepared nanocomposite single- and multi-layers consisting of a Nd₂Fe₁₄B-type hard phase and a soft α -Fe phase, by sputtering and subsequent heat treatment. The nanostructures of the multilayers can be well controlled by adjusting the thickness of the layers for the soft and hard phases. Annealing at appropriate temperatures leads to the formation of homogeneously dispersed soft- and hard-magnetic layers in the rare-earth multilayer film magnets. Remanence enhancement was observed in all the multilayer magnets, due to exchange coupling between the soft and hard phases. A maximum energy product of 192 kJ m⁻³ was achieved in the rare-earth nanostructured multilayers.

Acknowledgments

This work was supported by the US NSF under grant INT-9812082, and the US DOE, the National Natural Science Foundation of China under projects 59725103 and 50071062, the National 863 project under grant 2002AA302603 and the Science and Technology Commission of Shenyang.

References

- [1] Coehoorn R, de Mooji D B and Waard C D E 1989 *J. Magn. Mater.* **80** 101
- [2] Skomski R and Coey J M D 1993 *Phys. Rev. B* **48** 15812
- [3] Schrefl T, Krommüller H and Fidler J 1993 *J. Magn. Mater.* **127** L237
- [4] Kneller E F and Hawig R 1991 *IEEE Trans. Magn.* **27** 3588
- [5] Ding J, McCormick P G and Street R 1993 *J. Magn. Mater.* **124** 1
- [6] Manaf A, Buckley R A and Davies H A 1993 *J. Magn. Mater.* **128** 302
- [7] Withanawasam L, Hurphy A S, Hadjipanayis G C and Krause R F 1994 *J. Appl. Phys.* **75** 7065
- [8] Sun X K, Zhang J, Chu Y L, Liu W, Cui B Z and Zhang Z D 1999 *Appl. Phys. Lett.* **74** 1740
- [9] Al-Omari I A and Sellmyer D J 1995 *Phys. Rev. B* **52** 3441
- [10] Liu J P, Liu Y, Skomski R and Sellmyer D J 1999 *IEEE Trans. Magn.* **35** 3241
- [11] Shindo M and Ishizone M 1997 *J. Appl. Phys.* **81** 4444
- [12] Parhofer S, Wecker J, Kuhrt C and Gieres G 1996 *IEEE Trans. Magn.* **32** 4437
- [13] Parhofer S, Gieres G, Wecker J and Schultz L 1996 *J. Magn. Mater.* **163** 32
- [14] Yang C J and Kim S W 1999 *J. Magn. Mater.* **202** 311
- [15] Liu W, Zhang Z D, Liu J P, Li X Z, Sun X K and Sellmyer D J 2002 *J. Appl. Phys.* **91** 7890
- [16] Liu W, Zhang Z D, Liu J P, Chen L J, He L L, Liu Y, Sun X K and Sellmyer D J 2002 *Adv. Mater.* **14** 1832